Parametric analysis of 2D guided-wave photonic band gap structures

C. Ciminelli, F. Peluso and M. N. Armenise

Laboratorio di Optoelettronica, Politecnico di Bari, Via Orabona 4, 70125 Bari (Italy)
c.ciminelli@poliba.it

Abstract: The parametric analysis of the electromagnetic properties of 2D guided wave photonic band gap structures is reported with the aim of providing a valid tool for the optimal design. The modelling approach is based on the Bloch-Floquet method. Different lattice configurations and geometrical parameters are considered. An optimum value for the ratio between the hole (or rod) radius and the lattice constant does exist and the calculation demonstrated that it is almost independent from the etching depth, only depending on the lattice type. The results are suitable for the design optimisation of photonic crystal reflectors to be used in integrated optical devices.

OCIS codes: (999.9999) Photonic crystals; (230.3120) Integrated optics devices; (250.5300) Photonic integrated circuits

References and links

1. N. Ikeda, Y. Sugimoto, Y. Tanaka, K. Inoue, and K. Asakawa, "Low propagation posses in single-line-defect photonic crystal waveguides on GaAs membranes," IEEE J. Sel. Areas Commun. **23**, 1315-1320 (2005).
2. Y. Tanaka, T. Asano, R. Hatsuta, and S. Noda, "Analysis of a line-defect waveguide on a silicon-on-insulator two-dimensional photonic-crystal slab," J. Lightwave Technol. **22**, 2787-2792 (2004).
3. M. Koshiba, "Wavelength division multiplexing and demultiplexing with photonic crystal waveguide couplers," J. Lightwave Technol. **19**, 1970-1975 (2001).
4. J. Smajic, C. Hafner, and D. Erni, "On the design of photonic crystal multiplexers," Opt. Express **11**, 566-571 (2003), http://www.opticsexpress.org/abstract.cfm?URI=OPEX-11-6-566.
5. M. Loncar, T. Yoshie, Y. Qiu, P. Gogna, and A. Scherer, "Low-threshold photonic crystal laser," Proc. SPIE **5000**, 16-26 (2003).
6. M. Rattier, T. F. Krauss, J.-F. Carlin, R. Stanley, U. Oesterle, R. Houdrè, C. J. M. Smith, R. M. De La Rue, H. Benisty, and C. Weisbuch, "High extraction efficiency, laterally injected, light emitting diodes combining microcavities and photonic crystals," Opt. and Quantum Electron. **34**, 79-89 (2002).
7. H.-Y. Ryu, S.-H. Kwon, Y.-J. Lee, Y.-H. Lee, and J.-S. Kim, "Very-low-threshold photonic band-edge lasers from free-standing triangular photonic crystal slabs," Appl. Phys. Lett. **80**, 3476-3478 (2002).
8. K. Sakoda, "Low-threshold laser oscillation due to group-velocity anomaly peculiar to two- and three-dimensional photonic crystals," Opt. Express **4**, 481-489 (1999), http://www.opticsexpress.org/abstract.cfm?URI=OPEX-4-12-481.
9. A. Lupu, E. Cassan, S. Laval, L. El Melhaoui, P. Lyan, and J. M. Fedeli, "Experimental evidence for superprism phenomena in SOI photonic crystals," Opt. Express **23**, 5690-5696 (2004), http://www.opticsexpress.org/abstract.cfm?URI=OPEX-12-23-5690.
10. T. Baba, and M. Nakamura, "Photonic crystal light deflection devices using the superprism effect," IEEE J. Quantum Electron. **38**, 909-914 (2002).
11. R. Moussa, S. Foteinopoulou, L. Zhang, G. Tuttle, K. Guven, E. Ozbay, and C. M. Soukoulis, "Negative refraction and superlens behaviuor in a two-dimensional photonic crystal," Phys. Rev. B **71**, 085106 (2005).
12. E. Cubukcu, K. Aydin, and E. Ozbay, "Subwavelength resolution in a two-dimensional photonic-crystal-based superlens," Phys. Rev. Lett. **91**, 207401 (2003).
13. S. G. Johnson, S. Fan, P. R. Villeneuve, J. D. Joannopoulos, and L. A. Kolodziejski, "Guided modes in photonic crystal slabs," Phys. Rev. B **60**, 5751-5758 (1999).
14. C. Ciminelli, F. Peluso and M. N. Armenise, "Modeling and design of two-dimensional guided-wave photonic band-gap devices," J. Lightwave Technol. **23**, 886-901 (2005).

#8901 - $15.00 USD Received 26 September 2005; revised 7 November 2005; accepted 14 November 2005

15. C. Ciminelli, F. Peluso, M. N. Armenise and R. M. De La Rue, "Variable oblique incidence for tunability in a 2D guided wave photonic band gap filter," J. Lightwave Technol. (to be published).
16. C. Ciminelli, H. M. H. Chong, F. Peluso, M. N. Armenise and R. M. De La Rue, "High Q guided-wave photonic crystal extended microcavity" in *Proceedings of ECOC 2004*, Post deadline paper Th 4.2.6, 26-27.
17. T. D. Happ, A. Markard, M. Kamp, J.-L. Genter, and A. Forchel, "InP-based short cavity with 2D photonic crystal mirror," Electron. Lett. **37**, 428-429 (2001).
18. C. Ciminelli, F. Peluso, and M. N. Armenise, "2D guided-wave photonic band gap single and multiple cavity filters" in *Proceedings of 2005 IEEE/LEOS Workshop on Fibres and Optical Passive Components*, 404–409.
19. K. Sakoda, "Transmittance and Bragg reflectivity of two-dimensional photonic lattices," Phys. Rev. B **52**, 8992-9002 (1995).
20. D. Labilloy et al., "Diffraction efficiency and guided light control by two-dimensional photonic-bandgap lattices," IEEE J. Quantum Electron. **35**, 1045-1052 (1999).
21. W. Bogaerts, P. Bienstmann, D. Taillaert, R. Baets and D. De Zutter, "Out-of-plane scattering in photonic crystal slabs," IEEE Photon. Technol. Lett. **13**, 565-567 (2001).
22. J. D. Joannopoulos, R. D. Meade, and J. N. Winn, *Photonic Crystals: Molding the Flow of Light* (Princeton University Press, Princeton, New Jersey, 1995).

1. Introduction

Photonic crystals (PhCs) will promote the development of future optical integrated circuits where they could be exploited for the fabrication of different functional devices having high performance and very small size in a large number of applications. For some of them, such as waveguides [1, 2], mux/demux devices [3, 4], micro-cavity lasers [5] and led [6], the most important feature of photonic crystals is the existence of spectral regions, where the optical propagation is inhibited along specific directions or in whole space, namely photonic band gaps (PBGs). In other applications, such as band-edge laser [7, 8], superprism [9, 10] and superlens [11, 12], the dispersion properties (low group velocity, high chromatic dispersion, negative refraction) of this artificial materials are exploited.

2D guided-wave photonic crystals (PhCs) [13] are fabricated in conventional slab waveguide, providing total internal reflection for the confinement of the light along the direction perpendicular to the lattice plane. They can be realized by using e-beam lithography in III-V semiconductor hetero-structures or other material systems, such as silicon on insulator (SOI) and Al_xO_y/GaAs.

One of the most critical topic when dealing with these structures is their modelling for design purpose. It is needed to take into account the 3D variations of the refractive index to achieve a good level of accuracy. However, conventional methods like Finite Difference Time Domain Method, Finite Element Method and Transfer Matrix Method are very computationally expensive for 3D problems and not very suitable for a design procedure.

The Bloch-Floquet method has been successfully applied in the theoretical analysis of 2D guided-wave photonic crystals [14, 15]. It provides a rigorous modelling of perfectly periodic structures, allowing fast and accurate calculations of dispersion diagrams. This method can be also used for the approximated analysis of finite-size guided wave photonic crystals, with less time and memory consumption than the above mentioned methods.

In this paper, we report a detailed analysis, based on he Bloch-Floquet approach, of 2D guided-wave photonic crystal mirrors, fabricated in an Al_xO_y/GaAs slab waveguide operating at 1.55 μm. After a brief description of the theoretical method in Section 2, we carry out a parametric analysis in Section 3, which clarifies the influence of the different lattice configurations and geometrical parameters on the behaviour of the reflectors. Parametric curves which could be used for general purpose design are also reported.

2. Modelling approach

Let z and y be the periodic directions of a 2D PhC structure, as in Fig. 1.

#8901 - $15.00 USD Received 26 September 2005; revised 7 November 2005; accepted 14 November 2005

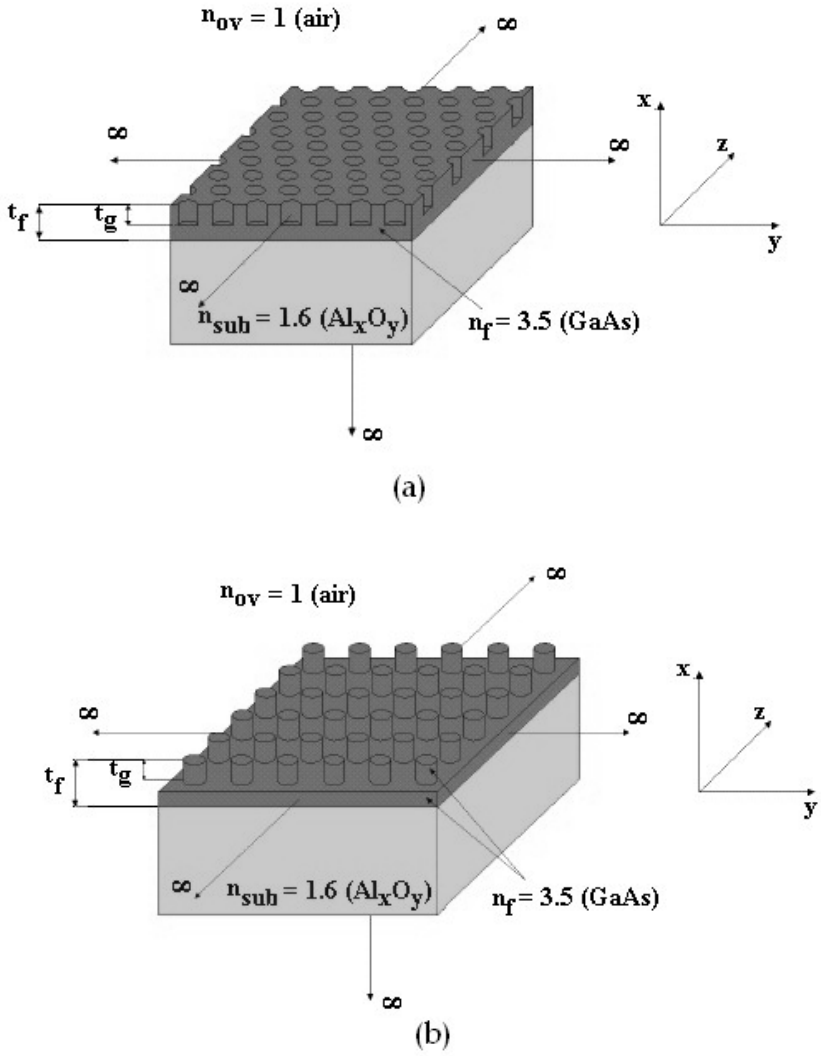

Fig. 1. Two different lattices. (a) periodic repetition of holes; (b) periodic repetition of rods.

Bloch's theorem allows expressing both electric and magnetic field as a sum of plane waves with amplitudes that are unknown functions of x in order to take into account the refractive index variations along the x-axis:

$$\mathbf{E,H} = \sum_{i,\mathbf{G}} \mathrm{E,H}_{i,\mathbf{G}}(x)\mathbf{a}_i e^{j(\mathbf{k}+\mathbf{G})\cdot\boldsymbol{\rho}} \tag{1}$$

where $\boldsymbol{\rho}$ is the position vector in the zy plane, $\mathbf{a}_i$ is the unitary vector along the i = x, y, or z axis, $\mathbf{k}$ represents the complex wavevector and $\mathbf{G}$ the generic reciprocal lattice vector given by:

#8901 - $15.00 USD Received 26 September 2005; revised 7 November 2005; accepted 14 November 2005

$$\mathbf{G} = m_1\mathbf{b}_1 + m_2\mathbf{b}_2 \tag{2}$$

being m_1, m_2 integer numbers, and $\mathbf{b}_1$, $\mathbf{b}_2$ the primitive vectors of the reciprocal lattice.

From Maxwell's equations we derive a linear differential equation system for the unknown field amplitudes. This system can be analytically solved inside each x-invariant layer, leading to the expression of E, $H_{i,\mathbf{G}}(x)$ as a linear combination of appropriate exponential functions having the eigenvalues of the considered layer as arguments [14].

By imposing the continuity of the z- and y-field components at each interface along x direction, a homogeneous system is obtained for the coefficients of the linear combination above mentioned in the semi-infinite layers (i.e. the cover and the substrate). After fixing the propagation direction and the frequency, the dispersion equation derived from the condition of existence of non-trivial solutions can be solved with respect to the complex amplitude of **k**, whose imaginary part will take into account both Bragg reflection and out-of-plane radiation. In this way the complete determination of the dispersion properties of infinite size PhCs can be carried out.

Bloch-Floquet modes of the perfectly periodic structures represent also a good expansion set for the field inside the finite length PhCs [14]. In the most simple case two independent anti-propagating Bloch modes are used:

$$\psi(x,\boldsymbol{\rho}) = a\psi^{+}(x,\boldsymbol{\rho}) + b\psi^{-}(x,\boldsymbol{\rho}) \tag{3}$$

where a and b are unknown coefficients and ψ represents a transversal field component.

A similar expression holds for the electromagnetic field inside unpatterned regions, but here the modes of the planar waveguide have to be considered. In the semi-infinite unpatterned regions, there is only one unknown coefficient, representing the reflection and transmission parameter at the input and output waveguide respectively.

A linear system for the unknown coefficients is obtained by imposing the continuity of the field at the interfaces between PhCs and unpatterned regions. The solution of this system gives the spectral response of several finite-length PhC regions separated by unpatterned zones [14, 15].

The calculation is very fast and the computational time does not depend on the length of PhCs but only on their number. The main disadvantage consists of not high accuracy in the evaluation of the maximum transmitted power because the scattering losses at the interfaces between patterned and unpatterned regions are not fully considered. However, a quite good agreement with experimental data has been observed through an appropriate comparison, thus validating our method as an efficient tool for optimising the design of 2D photonic band gap devices [16].

3. Parametric analysis

PhC reflectors are very attractive structures in integrated optics because of their capability in terms of high reflectance and small size and they can be used in several applications such as laser cavities [17] and optical filters [18].

In those applications where PhCs have to be used as mirror reflectors, only a directional (i.e. relevant to a certain direction) band gap is required. An optimised design is needed to maximize the power reflectance for a given number of hole (or rod rows), avoiding both out-of-plane radiation and in-plane diffraction. However, this is not a simple task if simulation techniques like FDTD, TMM, etc are used, because a large number of simulations, each for a different combination of lattice configuration (hole or rod lattice, triangular cell or square cell) and geometrical parameters (lattice constant, a, hole/rod radius, R, etching depth, t_g/t_f,) should

#8901 - $15.00 USD Received 26 September 2005; revised 7 November 2005; accepted 14 November 2005

be performed, thus involving a huge computational time. These methods are more suitable for an accurate post-design validation than for a design procedure.

The Bloch-Floquet method allows a fast computation of the propagation constants inside the periodic structures, for each propagation direction and free-space wavelength. A non vanishing imaginary part, α, can be calculated for the propagation constant, taking into account the attenuation due to Bragg reflection (evanescent modes, inside the forbidden bands) or out-of-plane radiation (leaky modes inside the out-of-plane radiation zones).

Bragg forbidden bands are the spectral region of interest for the optical mirrors. The attenuation coefficient α has a quasi-parabolic profile as a function of the wavelength inside the stop bands, reaching the maximum value around their centre and vanishing at the edges. For a given number of hole or rod rows, the reflectivity is a growing function of α.

On the contrary, if out-of-plane radiation takes place, an irregular spectral shape can be observed for the attenuation coefficient [14].

Along each propagation direction, these radiation effects are suppressed at wavelengths longer than a critical value $\lambda_{c,rad}$, which depends on the structure under investigation. In fact only for $\lambda < \lambda_{c,rad}$, the real part of the propagation constant, β, becomes less than the substrate wavenumber inside the first Brillouin zone and the optical field of the Bloch mode can no more be confined inside the waveguide core by total internal reflection. The Bragg forbidden band to be exploited for the optical reflector should belong to the spectral region where λ is greater than $\lambda_{c,rad}$, in order to avoid out-of-plane radiation losses.

Therefore, at least three performance parameters are very important in the design of a photonic crystal reflector, that are the peak value of the attenuation coefficient, the width of the first Bragg forbidden band and the distance between this region and the out-of-plane radiation zone.

In this section we analyse photonic crystal structures fabricated in an air/GaAs/Al_xO_y waveguide having a core thickness, t_f, of 100 nm and supporting only the propagation of the TE_0 mode at 1.55 μm. In our simulation we have considered a refractive index $n_f = 3.5$ inside the core and $n_{sub} = 1.6$ for the substrate. A single quasi-TE mode also exists in the photonic crystal under investigation, in a large spectral range around 1.55 μm [14]. This mode has the main component of the electric field along the y-axis (see Fig. 1) and according to the particular conditions, can propagate without losses, becomes evanescent due to Bragg reflection or radiate towards the substrate and/or the cover. We performed the calculation of dispersion diagrams for different values of the ratio between hole/rod radius and lattice constant at different etching depths, t_g, by using a numerical code based on the Bloch-Floquet modelling approach. Four different photonic crystal structures, deriving from the combination of two types of lattice, i.e. hole and rod repetition (see Fig. 1) and elementary cell symmetries, i.e. triangular or square (see Fig. 2), have been considered. In this way it has been possible to determine the optimal values for some important design parameters and to calculate parametric curves suitable for photonic crystal reflectors at 1.55 μm, in the waveguide system under investigation.

#8901 - $15.00 USD Received 26 September 2005; revised 7 November 2005; accepted 14 November 2005

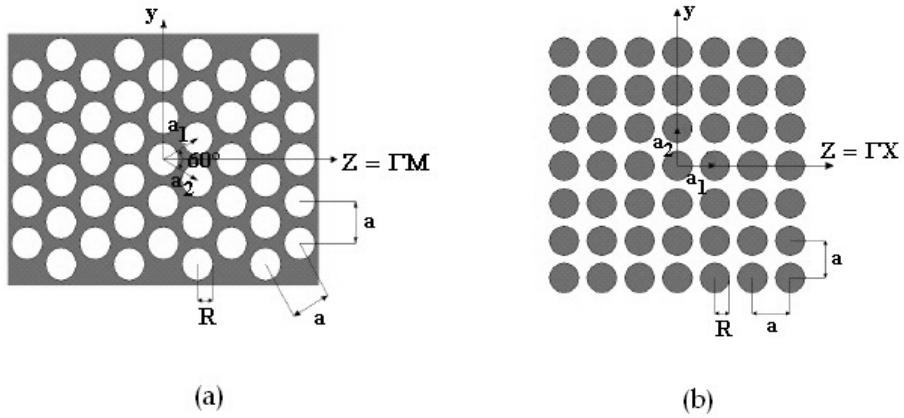

Fig. 2. Two different unit cell symmetries. (a) triangular; (b) square.

In the following subsections the influence on reflector performance of the R/a and t_g/t_f are discussed.

3. 1. Influence of the ratio R/a

In this subsection the influence of the R/a ratio on the performance of photonic crystals reflectors is investigated. We consider an etching depth equal to 60 % of the core thickness. The first step of the design procedure is the choice of the PhC orientation. Directions that minimize in-plane diffraction depending on the lattice configuration must be preferred in order to have a mirroring reflection. Let z be the incidence direction, perpendicular to the PBG mirrors. Diffraction is strongly dependent on the lattice period along the y-axis, Λ_y. In fact the y-component of the propagation wavevector of the p-th diffraction order can be expressed as:

$$\beta_{y,p} = p\frac{2\pi}{\Lambda_y} \tag{4}$$

If $\beta_{y,1}$ is greater than the propagation constant of the waveguide mode, β, at the desired wavelength, all diffraction orders with non zero p are evanescent and in-plane diffraction is completely suppressed. Therefore the best orientation is the one that minimizes Λ_y. In order to fulfil this condition PBG mirrors have to be perpendicular to the ΓX crystallographic direction for a square lattice, and to the ΓM direction for a triangular lattice [19, 20]. Moreover in this way the lowest frequency band gap is caused by hole (or rod) Bragg reflecting planes that are perpendicular to the z incidence direction [14], and, then, diffraction in the volume of the PhCs is avoided too.

All calculations have been performed by adjusting the lattice constant for each R/a value, in order to centre the first order Bragg bandgap region at the desired wavelength of 1.55 μm and to include that region in the lossless spectral zone (i.e. where the real part of k is greater than the substrate wavenumber $K_0 n_s$). The latter condition can be fulfilled only in planar waveguides with high index contrast between core and cladding, and allows an almost complete suppression of out-of-plane diffraction because the incident mode is coupled to a non-radiative Bloch mode of the lattice [21]. Therefore the efficiency of the Bragg reflection is fully represented by the attenuation coefficient α and the optimisation can be carried out by maximizing this parameter. Also the stopband width BW is related to the efficiency of Bragg

#8901 - $15.00 USD Received 26 September 2005; revised 7 November 2005; accepted 14 November 2005

reflection. For this reason it is expected that α and BW both increase or decrease by changing R/a.

In Fig. 3 the ratio between the bandgap width and the centre wavelength λ_0 = 1.55 μm, BW/λ_0, and the peak value of α inside the stop band, α_{max}, are depicted versus the R/a ratio.

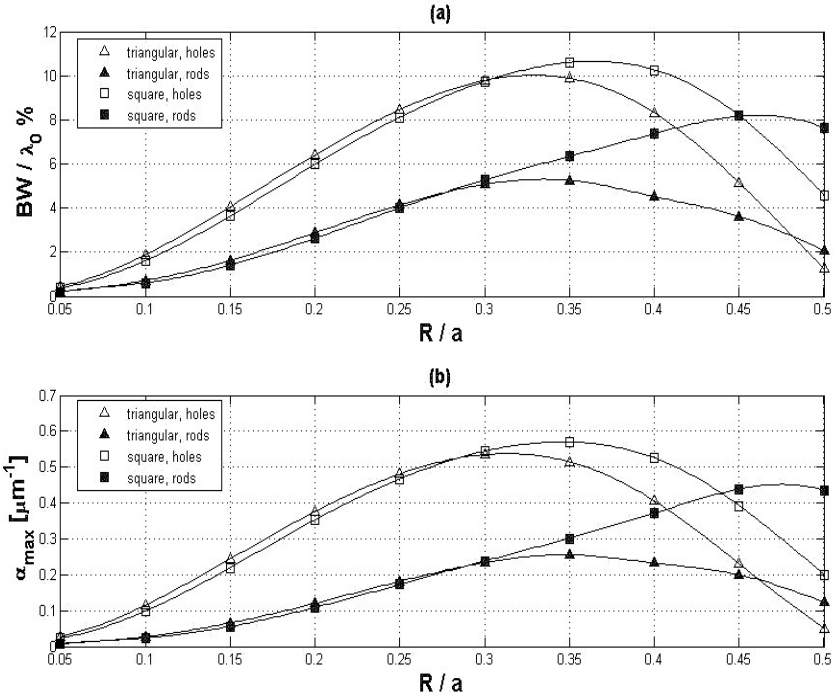

Fig. 3. BW/λ_0 versus R/a (a) and α_{max} versus R/a (b) for different photonic crystal structure in a 100 nm thick Al_xO_y/GaAs slab waveguide.

The results of the parametric analysis lead to the determination of an optimum value of the ratio R/a, $(R/a)_{opt}$, that maximizes both BW/λ_0 and α_{max}, thus minimizing the minimum length required for the PBG mirrors. This result was expected because both BW/λ_0 and α_{max} must be equal to zero at the internal edges R/a = 0 and R/a = 1, which correspond to the absence of any lattice inside the structure. From Fig. 3 it is clear that $(R/a)_{opt}$ is less than 0.5, which corresponds to holes (or rods) in contact. The optimum value depends on the PBG configuration but is almost unaffected by the etching depth. Calculated data are reported in Table 1.

Table 1. Optimum value of the ratio R/a, corresponding filling factor, $f_{opt,}$ relative width BW/λ_0 of the bandgap and peak attenuation coefficient α_{max} for different types of photonic crystals

Photonic crystal structure	**$(R/a)_{opt}$**	**f_{opt}**	**BW/λ_0 [%]**	**α_{max} [μm^{-1}]**
Triangular lattice, holes	0.325	0.383	10.0	0.54
Triangular lattice, rods	0.350	0.444	5.3	0.26
Square lattice, holes	0.350	0.384	10.7	0.57
Square lattice, rods	0.470	0.694	8.2	0.45

The largest bandgaps and attenuation coefficients have been obtained with photonic crystals made by a periodic repetition of holes and this confirms that our analysis is correct. In fact we are considering the propagation of a quasi-TE Bloch mode, i.e. with the main

#8901 - $15.00 USD Received 26 September 2005; revised 7 November 2005; accepted 14 November 2005

component of the electric field in the lattice plane, for which large Bragg bandgaps are favoured inside connected structures [22].

In Fig. 4 the approximated reflectivity, $|\rho|^2$, and transmittivity, $|\tau|^2$, at 1.55 μm for 15 reflecting hole rows (or rod rows) are illustrated.

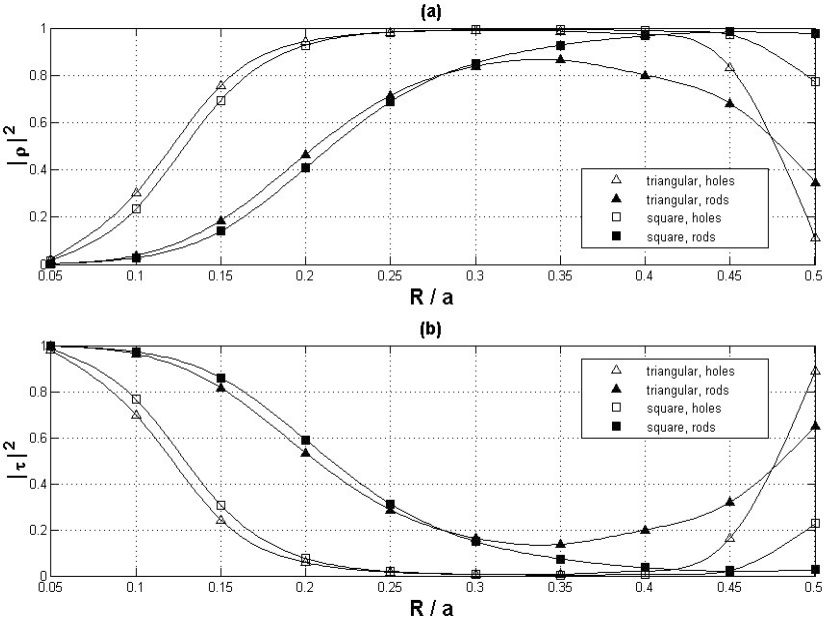

Fig. 4. Reflectance (a) and transmittance (b) at the centre of the stop band (λ_0 = 1.55 μm) versus R/a for different photonic crystal structures in a 100 nm thick Al_xO_y /GaAs slab waveguide (15 hole/rod rows).

The behaviour in Fig. 4(a) is similar to that one in Fig 3(b), being the reflectivity near the centre of the Bragg stopband a growing function of the peak attenuation coefficient.

Then, we have considered the influence of R/a on the out-of-plane radiation. In Fig. 5(a) the relative distance between the stopband centre λ_0 and the cut-off wavelength for the out-of-plane radiation $\lambda_{c,rad}$ is depicted as a function of R/a. A different behaviour holds for hole and rod lattices. Out-of-plane radiation takes place when a critical fraction of the free space wavelength is contained inside the air zones of unit cells, where the optical field tends to diffract towards the cover and the substrate. For hole lattices, increasing the R/a ratio causes a growth of the percentage of air in each unit cell. The cut-off wavelength for out-of-plane radiation increases and becomes closer to the centre of the bandgap as R/a grows. On the contrary, for rods lattices, the percentage of air in the unit cells is a decreasing function of R/a. Thus, a positive slope of the curves in Fig. 5(a) can be observed, which means that $\lambda_{c,rad}$ becomes shorter and more distant from λ_0, as R/a grows.

In Fig. 5(b) we report the ratio between the half width of the stopband and the distance $|\lambda_0 - \lambda_{c,rad}|$, which represents the percentage of the spectral region $[\lambda_{c,rad}, \lambda_0]$ covered by the Bragg bandgap. If this parameter is less than 100%, a lossless propagation zone between the out-of-plane region and the forbidden band does exist and it measures the separation between these two spectral zones. This parameter is very useful when the entire Bragg bandgap has to be exploited for the reflector performance and out-of-plane radiation losses need to be avoided at any wavelength in the bandgap.

#8901 - $15.00 USD Received 26 September 2005; revised 7 November 2005; accepted 14 November 2005

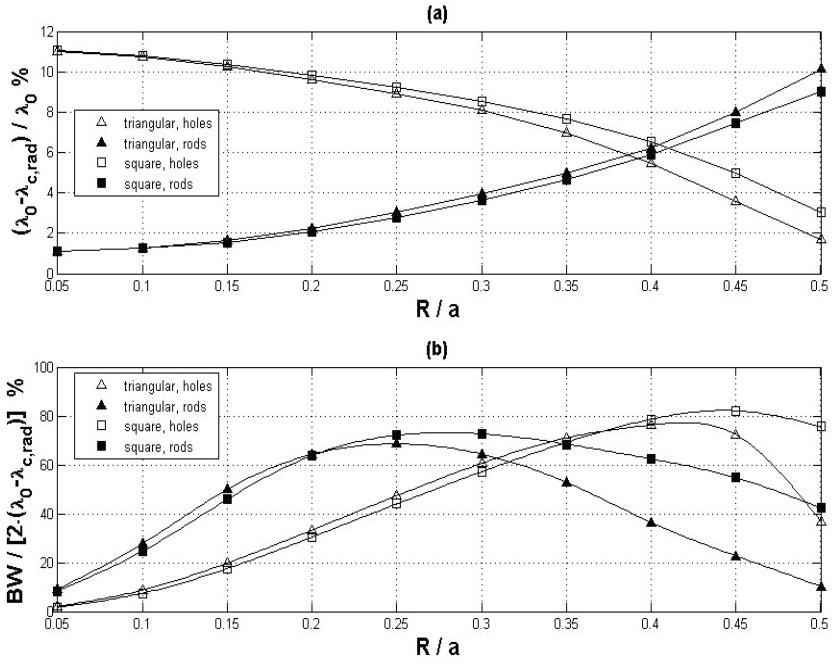

Fig. 5. $(\lambda_0 - \lambda_{c,rad})/\lambda_0$ (a) and relative percentage (b) versus R/a for different photonic crystal structures in a 100 nm thick Al_xO_y/GaAs slab waveguide.

For the structure under investigation, when R/a is less than 0.5, a separation region always exists and the Bragg bandgap is fully included in the lossless zone. However, there is a critical value of R/a where the width of the separation region is minimized (at the maximum of the curves in Fig. 5(b)), which could be a condition making easy the coupling to the radiation modes in finite-size photonic crystal reflectors.

3. 2. Influence of the etching depth t_g/t_f with R/a = constant

The etching depth is defined as the ratio between the hole (or rod) height (t_g) and the core thickness (t_f). In this subsection the performance of photonic crystal reflectors are investigated for different values of this parameter, ranging from 5% to 95%, so considering structures un-etched in the substrate. In each simulation the lattice constant has been chosen to obtain λ_0 = 1.55 μm as the centre wavelength of the first order Bragg bandgap, while the R/a ratio has been selected in order to maximise the stopband width and the peak attenuation coefficient at t_g/t_f = 60%, according to Table 1. Moreover, as in the previous subsection, the propagation direction is ΓM for triangular lattices and ΓX for square lattices.

In Fig. 6(a) the relative width of the stopband is represented. The increase of the etching depth causes a growth of the strength of the interaction between optical field and lattice film, leading to larger Bragg bandgap, as reported in Fig. 6(a). However, the percentage of air zones inside the structure also grows, causing the field to be less confined inside the core of the slab waveguide, which has an opposite effect on the bandgap. This phenomenon gives rise to the saturation of the gap width in the case of the triangular lattice of dielectric rods.

In Fig. 6(b) the ratio between the half width of the bandgap and the distance $|\lambda_0 - \lambda_{c,rad}|$ is reported. It clear that the growth of the etching depth makes the out-of-plane radiation zone closer to the first order stopband, i.e. the ratio in Fig. 6(a) tends to 100%. For each type of photonic crystals, a critical value of etching depth does exist which gives rise to the superimposition between these spectral regions. Clearly, for those applications where the

#8901 - $15.00 USD Received 26 September 2005; revised 7 November 2005; accepted 14 November 2005

whole Bragg bandgap has to be exploited, the etching depth should be less than this critical value, in order to avoid high radiation losses. From Fig. 6(b) it is evident that the triangular lattice of rods has the worse behaviour with a critical etching depth near to 80%.

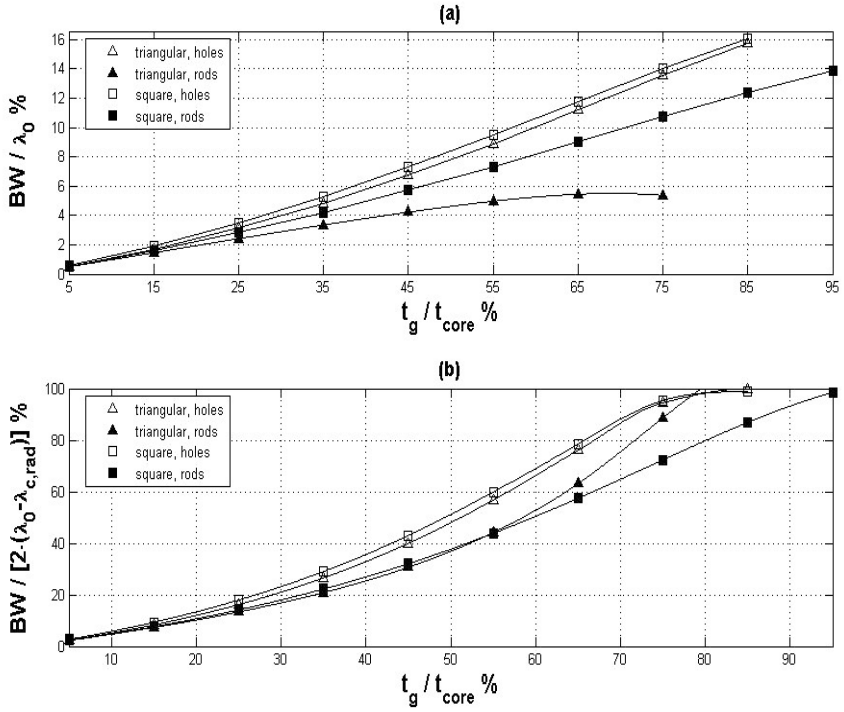

Fig. 6. BW/λ_0 % (a) and BW/[2 - (λ_0 – $\lambda_{c,rad}$)] (b) versus etching depth for different photonic crystal structure in a 100 nm thick Al_xO_y/GaAs slab waveguide.

In Fig. 7(a) the peak value of the attenuation coefficient inside the Bragg bandgap is reported as a function of the etching depth. The behaviour is very similar to that one in Fig. 6(a). In figures 7(b) and 7(c) the reflectivity and transmittivity at 1.55 μm obtained by considering 15 reflecting rows of holes or rods are illustrated.

#8901 - $15.00 USD Received 26 September 2005; revised 7 November 2005; accepted 14 November 2005

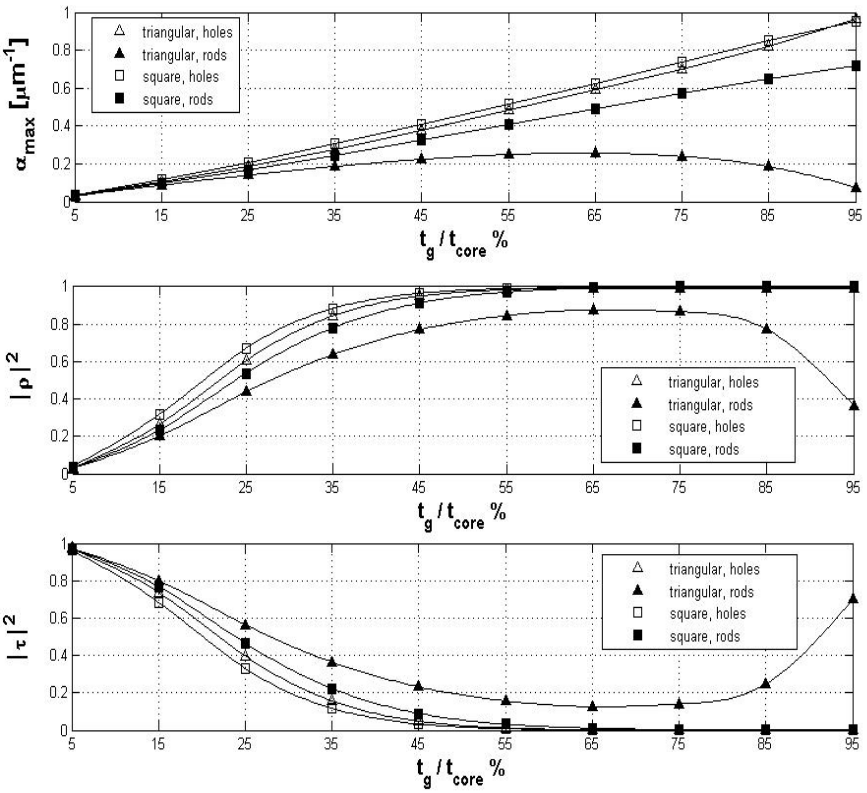

Fig. 7. Peak attenuation coefficient in the forbidden band (a), reflectance at λ_0 (15 hole/rod rows) (b), transmittance at λ_0 (15 hole/rod rows) (c) as function of the etching depth t_g/t_f for different photonic crystal structures in a 100 nm thick Al_xO_y/GaAs slab waveguide.

3. 3. Influence of the etching depth t_g/t_f with R/a variable

In this subsection we discuss the variation with R/a of the most important performance parameters at different etching depth values. The analysis is carried out for each of the four different types of photonic crystals under investigation. The combination of the effects of the design parameters R/a and t_g/t_f is analysed, thus giving a complete description of the behaviour of these structures when used as optical reflectors. The results are reported in s 8 – 11. In particular, Figs 8, 9, 10, and 11 illustrate the behaviour of the parameters BW/λ_0 %, (λ_0 – $\lambda_{c,rad}$)/λ_0 %, $|\rho|^2$ and $|\tau|^2$ as functions of the ratio R/a by changing the etching depth for triangular lattice of holes, triangular lattice of rods, square lattice of holes and square lattice of holes, respectively.

#8901 - $15.00 USD Received 26 September 2005; revised 7 November 2005; accepted 14 November 2005

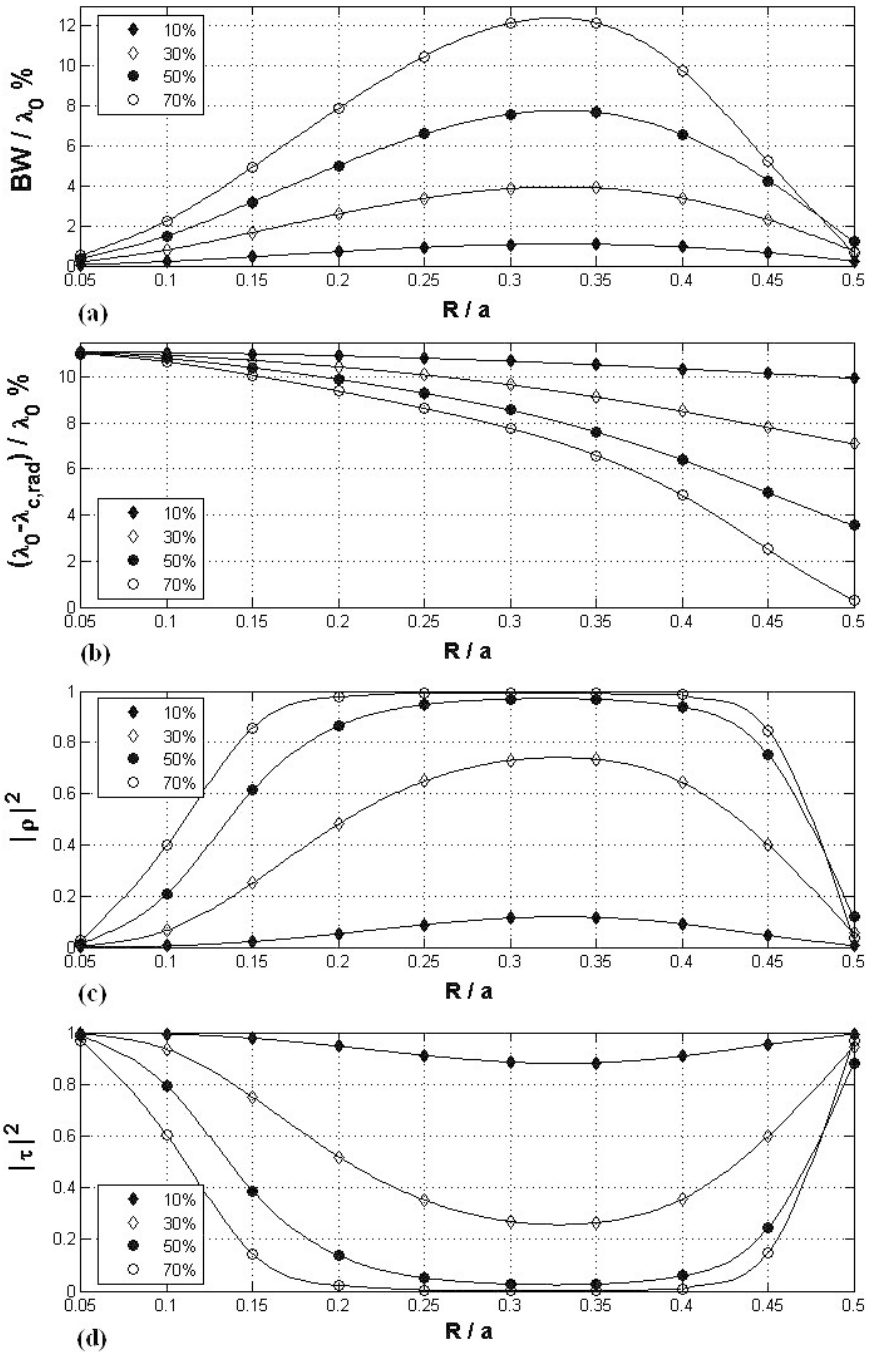

Fig. 8. BW/λ_0 % (a), ($\lambda_0 - \lambda_{c,rad}$)/$\lambda_0$ (b), reflectance at λ_0 = 1.55 μm (15 hole rows) (c), transmittance at λ_0 (15 hole rows) (d) as functions of the ratio R/a at different etching depths t_g/t_f for a triangular lattice of holes in a 100 nm thick Al_xO_y/GaAs slab waveguide.

#8901 - $15.00 USD Received 26 September 2005; revised 7 November 2005; accepted 14 November 2005

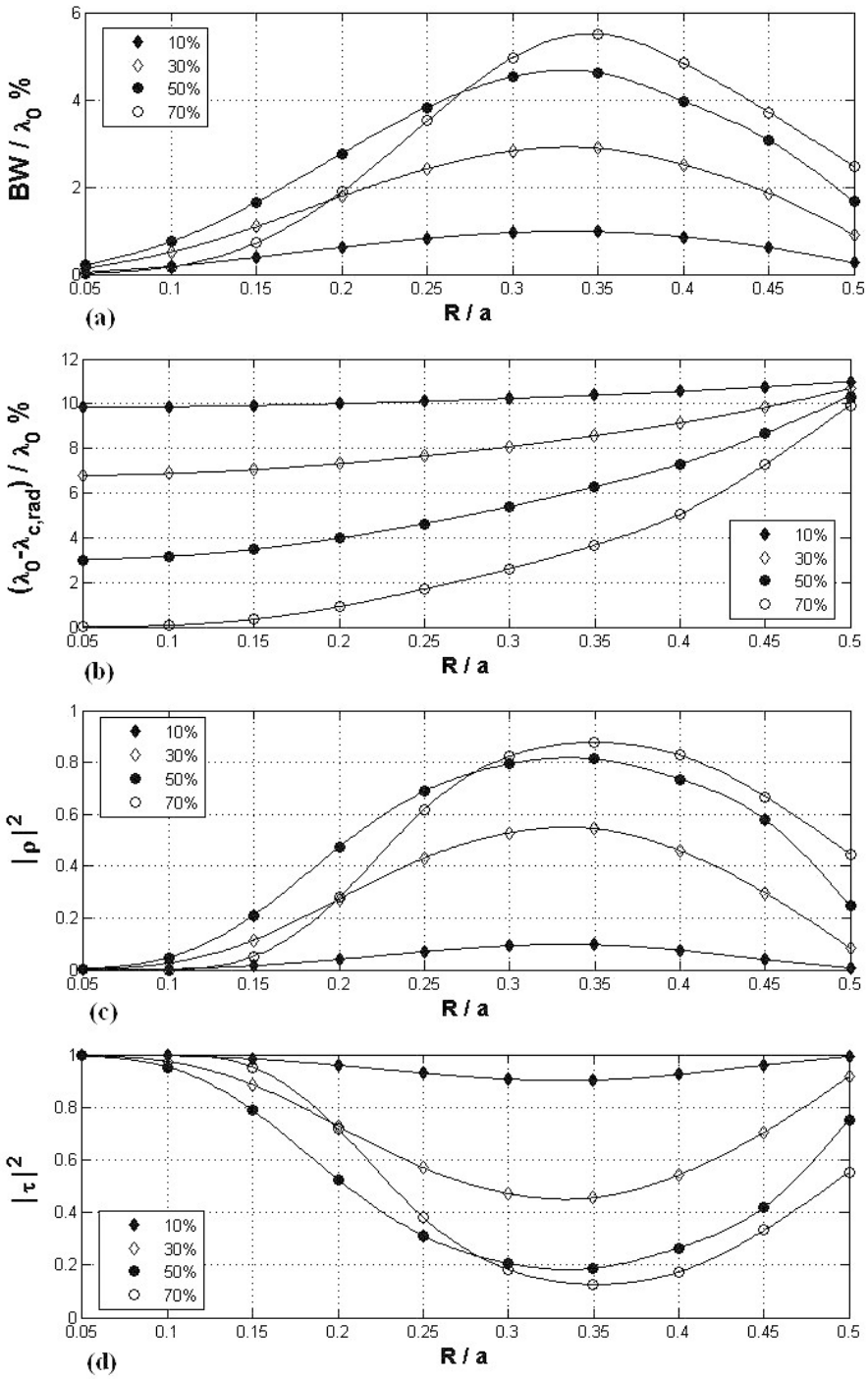

Fig. 9. BW/λ_0 % (a), ($\lambda_0 - \lambda_{c,rad}$)/$\lambda_0$ (b), reflectance at λ_0 = 1.55 μm (15 rod rows) (c), transmittance at λ_0 (15 rod rows) (d) as functions of the ratio R/a at different etching depths t_g/t_f for a triangular lattice of rods in a 100 nm thick Al_xO_y/GaAs slab waveguide.

#8901 - $15.00 USD Received 26 September 2005; revised 7 November 2005; accepted 14 November 2005

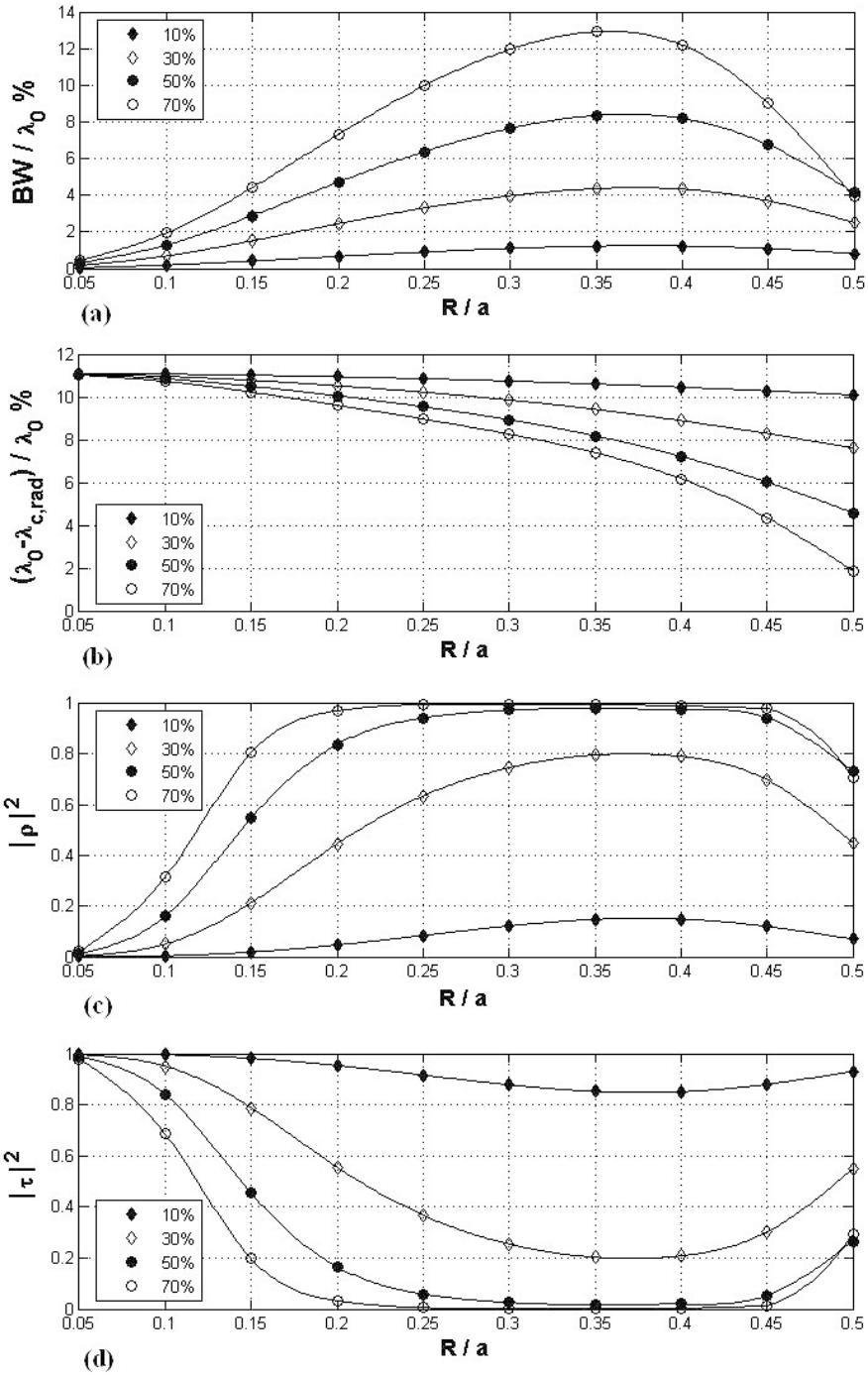

Fig. 10. BW/λ_0 % (a), $(\lambda_0 - \lambda_{c,rad})/\lambda_0$ (b), reflectance at λ_0 = 1.55 μm (15 hole rows) (c), transmittance at λ_0 (15 hole rows) (d) as functions of the ratio R/a at different etching depths t_g/t_f for a square lattice of holes in a 100 nm thick Al_xO_y/GaAs slab waveguide.

#8901 - $15.00 USD Received 26 September 2005; revised 7 November 2005; accepted 14 November 2005

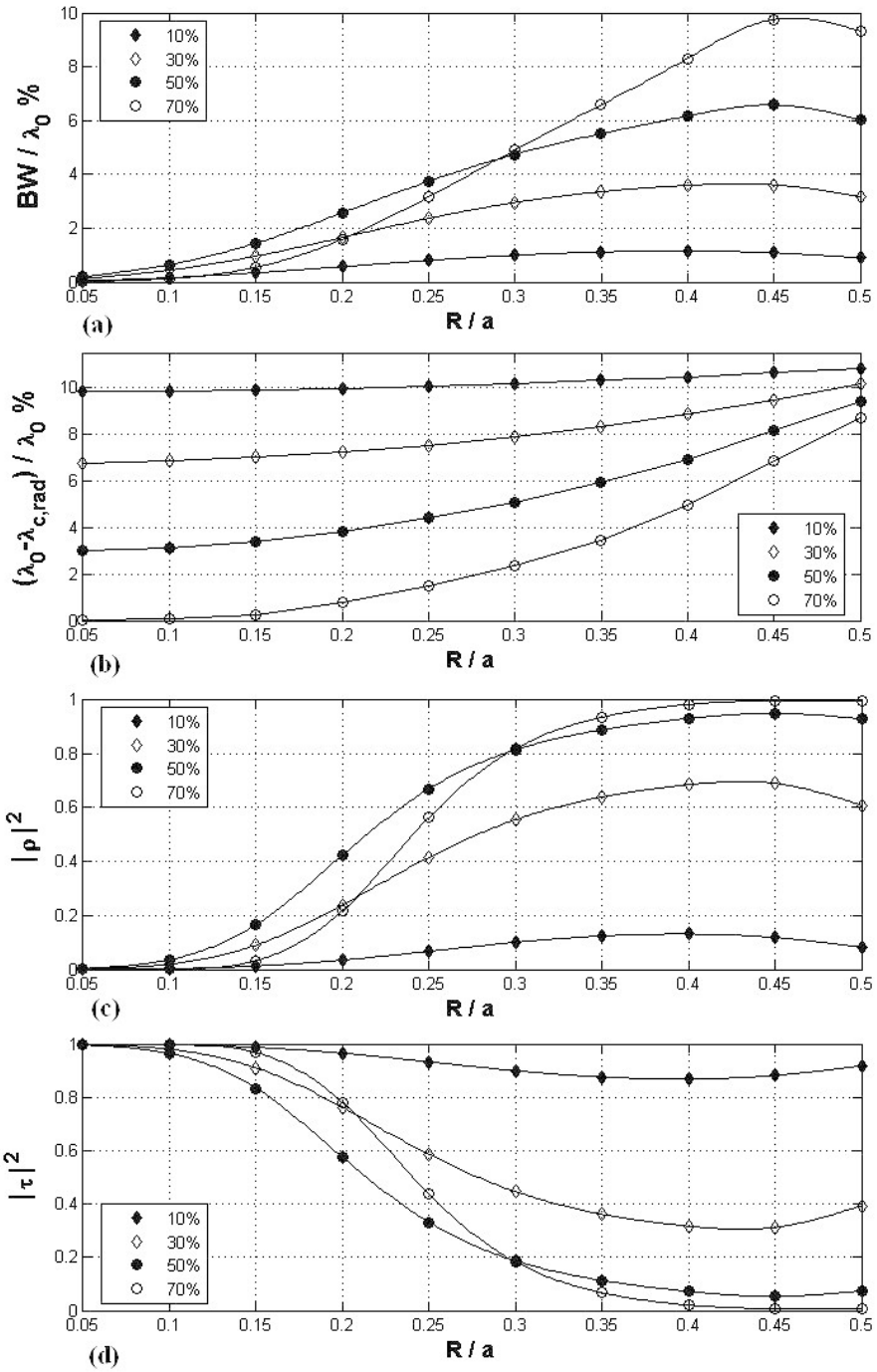

Fig. 11. BW/λ_0 % (a), ($\lambda_0 - \lambda_{c,rad}$)/$\lambda_0$ (b), reflectance at λ_0 = 1.55 μm (15 rod rows) (c), transmittance at λ_0 (15 rod rows) (d) as functions of the ratio R/a at different etching depths t_g/t_f for a square lattice of rods in a 100 nm thick Al_xO_y/GaAs slab waveguide.

The Bragg bandgap width and the centre wavelength reflectivity (transmittivity) are not monotonic functions of the etching depth. In fact, as pointed out also in the previous

#8901 - $15.00 USD Received 26 September 2005; revised 7 November 2005; accepted 14 November 2005

subsection, the increase of t_g/t_f causes a stronger Bragg reflection only until the decrease of the field confinement inside the core gives rise to a weak interaction between optical mode and lattice. This opposite effect is favoured when a large percentage of air in the unit cells does exist. For this reason a decrease of both the Bragg bandgap width and the centre wavelength reflectivity corresponding to an increase of the etching depth from 50% to 70%, can be observed only for R/a as high as 0.5, for hole lattices (see Figs. 8(a), 8(c), 10(a), 10(c)) and only at small values of R/a for rod lattices (see Figs. 9(a), 9(c), 11(a), 11(c)). The value of t_g/t_f which gives rise to the maximum Bragg bandgap width and peak reflectivity depends on the choice of the ratio R/a.

On the contrary, it is clear from Figs. 8-11 that the optimum value of the ratio R/a, corresponding to the maximum of the curves for the Bragg bandgap (see Figs. 8(a), 9(a), 10(a), 11(a)), does not significantly change with the etching depth. It means that it is possible to make the best choice for R/a independently from the etching depth and this is one of the most important results of the present analysis.

It can be also observed from Figs. 8-11 that, for planar waveguide under investigation, the best photonic crystal mirrors are obtained with the hole square lattice, oriented along the ΓX symmetry direction. In fact this structure shows the largest stopband, the highest peak attenuation coefficient and the highest reflectivity at centre wavelength, keeping the first order Bragg bandgap in the lossless spectral region.

In Fig. 12 we have reported the dispersion diagrams of the above mentioned structure, with the optimum value of 0.35 for R/a (see Table 1). A clear separation between radiation zone and Bragg bandgap does exist with an etching depth is less than 90%.

#8901 - $15.00 USD Received 26 September 2005; revised 7 November 2005; accepted 14 November 2005

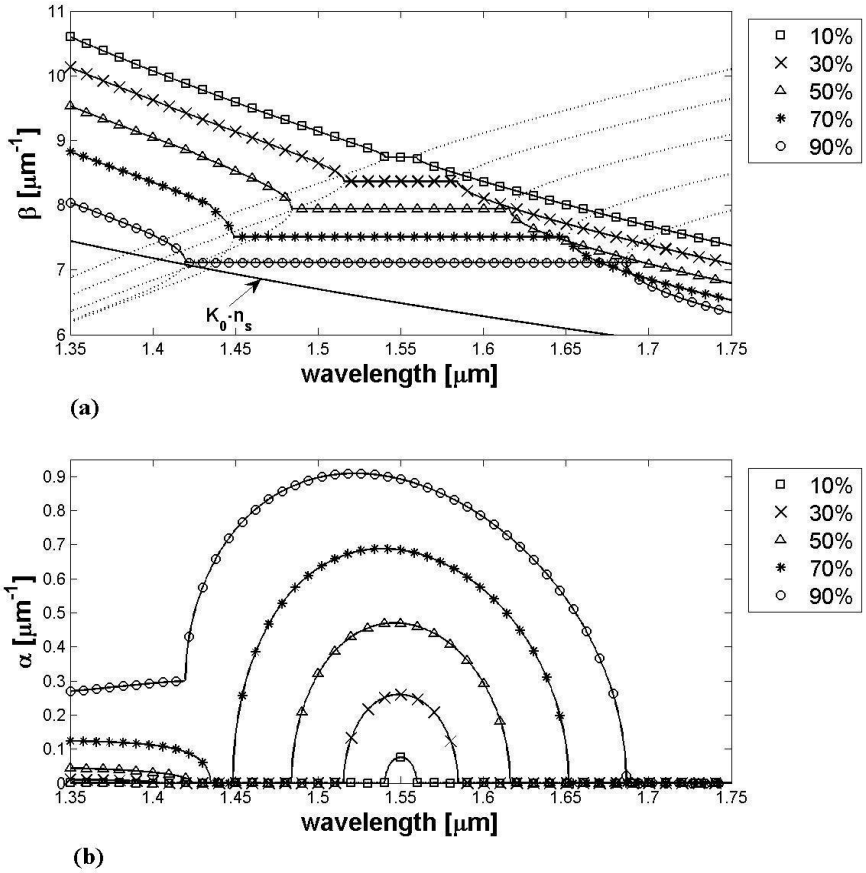

Fig. 12. Dispersion curves of photonic crystals consisting on a square pattern of holes, evaluated along the ΓX direction for four different etching depths. The ratio R/a is equal to 0.35 and the lattice constant a is adjusted to have a centre wavelength λ_0 = 1.55 μm in each case: (a) phase constant; (b) attenuation coefficient.

4. Conclusions

We have proposed a parametric analysis of photonic crystal structures fabricate in Air/GaAs/Al_xO_y planar waveguides, supporting single mode propagation at 1.55 μm, by using Bloch-Floquet modelling approach with the aim of identifying the right conditions for the optimum design. The results can be exploited for the design of optical reflectors at the centre wavelength of 1.55 μm and could also be extended to different centre wavelengths by considering the proper scale factor for all the geometrical parameters, if the material dispersion is not dominant. Our analysis clarifies the influence of the different design parameters and types of lattice on the overall performance and gives a physical insight. We have determined some design rules for this kind of structures. The existence of an optimum value for the ratio between the hole or rod radius and the lattice constant, which is almost independent from the etching depth and depends only on the type of lattice, is one of the most important result. Bloch-Floquet method confirms itself as a powerful tool for optimising the design of PBG devices, allowing the fast and rigorous computation of dispersion diagrams and the approximated calculation of reflectivity and transmittivity for finite size structures.

#8901 - $15.00 USD Received 26 September 2005; revised 7 November 2005; accepted 14 November 2005

Acknowledgments

The authors acknowledge the financial support of the Italian Education Ministry under Contract F.I.R.B. n. RBNE01KZ94 on "Photonic Devices in $LiNbO_3$."

#8901 - $15.00 USD Received 26 September 2005; revised 7 November 2005; accepted 14 November 2005